RGS22 inhibits pancreatic adenocarcinoma cell migration through the G12/13 α subunit/F-actin pathway

YANQIU HU[1*], JUN XING[3*], LING CHEN[2], YING ZHENG[4] and ZUOMIN ZHOU[2]

[1]Reproductive Medicine Center, Subei People's Hospital, Yangzhou University, Yangzhou, Jiangsu 225001; [2]Laboratory of Reproductive Medicine, Nanjing Medical University, Nanjing, Jiangsu 210029; [3]Reproductive Medicine Center, The Affiliated Drum Tower Hospital of Nanjing University Medical School, Nanjing, Jiangsu 210008; [4]Department of Histology and Embryology, Medical College, Yangzhou University, Yangzhou, Jiangsu 225001, P.R. China

Received June 15, 2015; Accepted July 27, 2015

DOI: 10.3892/or.2015.4209

Abstract. Pancreatic cancer is characterized by the potential for local invasion, allowing it to spread during the early developmental stages of the disease. Regulator of G protein signaling 22 (RGS22) localizes to the cytoplasm in pancreatic adenocarcinoma tissue. We overexpressed RGS22 in the human pancreatic cancer cell line BXPC-3. Cells that overexpressed RGS22 had much lower wound-healing rates and greatly reduced migration compared to the control cells. Conversely, cells in which RGS22 expression had been downregulated had higher wound-healing rates and migration than the control cells. These results confirmed that RGS22 expression suppresses pancreatic adenocarcinoma cell migration. Pull-down and coimmunoprecipitation assays revealed that RGS22 had specific interactions with the heterotrimeric G protein G12 α subunit (GNA12) and GNA13 in the cells. We also demonstrated that in the presence of higher RGS22 expression, the cell deformation and F-actin formation caused by lysophosphatidic acid treatment, is delayed. Constitutively active Gα subunits did not accelerate GTP hydrolysis to GDP. We did not investigate the function of RGS22 as a negative regulator of heterotrimeric G12/13 protein signaling. Our data demonstrate that RGS22 acts as a tumor suppressor, repressing human pancreatic adenocarcinoma cell migration by coupling to GNA12/13, which in turn leads to inhibition of stress fiber formation.

Correspondence to: Dr Yanqiu Hu, Reproductive Medicine Center, Subei People's Hospital, Yangzhou University, 98 Nantong West Road, Yangzhou, Jiangsu 225001, P.R. China
E-mail: yanqiuhu@yahoo.com

Professor Zuomin Zhou, Laboratory of Reproductive Medicine, Nanjing Medical University, 140 Hanzhong Road, Nanjing, Jiangsu 210029, P.R. China
E-mail: zhouzm@njmu.edu.cn

[*]Contributed equally

Key words: regulator of G protein signaling 22, pancreatic adenocarcinoma, migration, Gα12/13, F-actin

Introduction

Pancreatic cancer is a disease with a dismal outlook. Pancreatic adenocarcinoma is among the leading causes of cancer-related mortality worldwide (1), and the 1- and 5-year survival rates are <25 and <6%, respectively. Pancreatic cancer is characterized by the potential for local invasion, which allows it to spread during the early developmental stages of the disease. Therefore, there is an urgent need to discover novel early diagnostic biomarkers and to identify new therapeutic strategies (2). However, the molecular mechanisms underlying the high tumorigenicity of pancreatic cancer are not well known.

It was recently reported that regulator of G protein signaling 22 (RGS22) is specifically expressed in the testis during different stages of development (3). Furthermore, we previously showed that RGS22 is specifically expressed in adenocarcinoma and squamous carcinoma. In particular, we observed that RGS22 localized to the cytoplasm in pancreatic adenocarcinoma tissues. RGS22 also acts as a tumor suppressor, repressing the metastasis of epithelial cancer cells (4).

Tumor metastasis involves a series of complex host-tumor interactions (5). Tumor cell extravasation into the surrounding tissue is considered a rate-limiting step in metastasis (6,7) that involves the active migration of tumor cells across the endothelial barrier, and penetration through the underlying basement membrane. Tumor cell interaction with the basement membrane is a 3-step process: cell attachment, matrix dissolution, and migration (8). Previously, we found that tumor cells with high RGS22 expression have decreased metastatic potential and local invasiveness when compared to the control cells, but have similar adherence ability to various basement membrane substrates (4). Therefore, whether RGS22 is involved in pancreatic adenocarcinoma cell migration requires investigation.

Several classes of proteins are involved in metastasis. The heterotrimeric G protein G12 α subunit (GNA12) signaling promotes the migration of prostate (9) and breast cancer cells (10), and lysophosphatidic acid (LPA)-induced ovarian cancer cell migration *in vitro* (11). GNA12 signaling promotes metastasis by stimulating cells to become invasive within the

primary tumor. GNA13, has also been shown to stimulate cell migration in addition to inducing oncogenic transformation (12). The RGS22 RGS protein (a diverse family of proteins that regulate heterotrimeric G protein signaling negatively), interacts with GNA12/13 and GNAq in the testis (3). Therefore, the Gα subunit through which RGS22 demonstrates significant ability to inhibit cancer cell migration, should also be further studied.

Materials and methods

Plasmids and constructs. We constructed a plasmid containing LZRsPBMN-Z complementary DNA (cDNA) via a retrovirus vector according to the following protocols. The RGS22 open reading fragment (from 21 to 3783 bp) was PCR-amplified from a pTriplEx2-RGS22 plasmid using a forward, 5'-GGGGGTCGA CAAGCTTGGCATGCCCGAGAAGACG-3'; containing a *Hin*dIII site and reverse primer, 5'-GGGGCTCGAGCTTCTG GCTGCTGTGGGC-3'; containing an *Xho*I site. The RGS22 fragments were purified and digested with *Hin*dIII and *Xho*I. The LZRsPBMN-Z vector was also digested with *Hin*dIII and *Xho*I, and ligated with the RGS22 fragments. The RGS22 sequence in the construct was confirmed by DNA sequencing. Green fluorescent protein (GFP) cDNA was inserted into the vector as the control.

We purchased a pSilencer 2.1-U6 neo vector for RGS22 RNAi from Ambion (Austin, TX, USA). A 19-mer hairpin with a loop and 3' terminal uridine tract efficiently induces RNAi of the target gene. For each target gene, we designed complementary 55-60-mer oligonucleotides with 5' single-stranded overhangs for ligation into the pSilencer neo vectors. The oligonucleotides encoded 19-mer hairpin sequences specific to the mRNA target, a loop sequence separating the two complementary domains, and a polythymidine tract to terminate transcription. Therefore, we designed the following primers: 484 forward, 5'-GATCCGTCCGGCATGAATTTCAC ATTCAAGAGATGTGAAATTCATGCCGGACTTTTTTGG AAA-3' and reverse, 5'-AGCTTTTCCAAAAAAGTCCGGC ATGAATTTCACATCTCTTGAATGTGAAATTCATGCCG GACG-3'; 3313 forward, 5'-GATCCGGAGTTAGGACCATAT GTATTCAAGAGATACATATGGTCCTAACTCCTTTTTTG GAAA-3' and reverse, 5'-AGCTTTTCCAAAAAAGGAGTT AGGACCATATGTATCTCTTGAATACATATGGTCCTAAC TCCG-3'. The kit also contained pSilencer-Neg, in which the inserted sequence does not match human, mouse, or rat genomes, and was used as the negative control. We annealed the hairpin small interfering RNA (siRNA) template oligonucleotides, and then ligated the annealed siRNA templates into the pSilencer vector according to the instruction manual.

Constructs each containing human GA12 Q231L, GA13 Q226L and GAq Q209L in the pcDNA3.1 vector were purchased from the University of Missouri-Rolla cDNA Resource Center (Rolla, MO, USA). The mutations reduce GTPase activity, resulting in a constitutively active phenotype.

Cell culture and transfection. LZRsPBMN-Z-RGS22 and LZRsPBMN-Z-GFP plasmids were transfected using a transfection kit (Invitrogen, San Diego, CA, USA) into BXPC-3 cells purchased from the Institute of Cell, Chinese Academy of Science (Shanghai, China). Briefly, we seeded $4x10^5$ cells/well in a 6-well plate the day before transfection and cultured them overnight. Transfection was performed using Lipofectamine 2000 according to the manufacturer's protocol (Invitrogen). After transfection, cells were cultured in RPMI-1640 medium (Invitrogen, Rockville, MD, USA) supplemented with 10% (v/v) fetal calf serum (FCS), 100 μg/ml streptomycin, and 100 μg/ml penicillin (pH 7.2-7.4) in a humidified incubator containing 5% CO_2 at 37˚C, and selected with 1 μg/ml puromycin for one week. We confirmed RGS22 expression in the cells by western blotting.

We transfected pSilencer-Neg, pSilencer-484 and pSilencer-3313 into BXPC3-LZR-RGS22 cells using an Invitrogen transfection kit. We selected the cell lines using 200 μg/ml G418 for two weeks. We confirmed RGS22 expression in the cells (LZR-RGS22-Neg, LZR-RGS22-484, LZR-RGS22-3313) by western blotting.

We transfected constructs, each containing human Gα12 Q231L, Gα13 Q226L and Gαq Q209L in the pcDNA3.1 vector into BXPC3-LZR-RGS22 cells using an Invitrogen transfection kit.

Western blotting. Lysates of BXPC3-LZR-GFP and BXPC3-LZR-RGS22 cells or LZR-RGS22-Neg, LZR-RGS22-484 and LZR-RGS22-3313 cells were subjected to sodium dodecyl sulfate-polyacrylamide gel electrophoresis (SDS-PAGE) and immunoblot analysis. Proteins were transferred to 0.2-μm nitrocellulose membranes and blotted with antibody to RGS22 (3) or the control tubulin (Abcam, Cambridge, UK). We detected the proteins using secondary antibodies (Beijing Zhongshan Biotechnology, Beijing, China). Specific proteins were detected using an enhanced chemiluminescence substrate; bands were analyzed with AlphaImager™ (Amersham, Piscataway, NJ, USA).

Wound-healing assay. Cells were cultured to confluence in 60-mm diameter dishes and synchronized with serum-free medium for 24 h. A wound was created by abrasion with a sterile pipette tip, and the cell layer washed twice to remove non-adherent cells. Cells were cultured in medium containing 10% FCS for 6 h, and wound healing was visualized using a Nikon TE2000 microscope (Nikon, Melville, NY, USA). The cell-free surface area was calculated using Zeiss AxioVision v4.5 software (Carl Zeiss, Oberkochen, Germany). The experiments were repeated three times for reproducibility. Data are presented as the ratio of cell-covered surface area to initial cell-free surface area.

Cell migration assay. We performed the cell migration assay using a Transwell chamber with 8-μm pore, 24-mm wide polycarbonate filters (Coaster, Cambridge, MA, USA). Cells ($5x10^5$) were resuspended in serum-free culture medium, plated onto the upper chamber, and allowed to migrate for 12 h through the filter into the lower chamber. The bottom wells were filled with culture medium supplemented with 10% FCS or 0.1% BSA. Non-migrating cells were removed from the upper chamber with a cotton swab, the filters were stained with hematoxylin, and the migrating cells adhering to the underside of the filter counted in five random areas under a light microscope. The experiments were repeated three times.

In vitro pull-down assay and co-immunoprecipitation (Co-IP). LZRsPBMN-Z-RGS22 BXPC-3 cells were sonicated and lysed in 20 mM Tris-HCl (pH 7.5) containing 5 mM EDTA, 100 mM NaCl, 5 mM benzamine, 0.2% Triton X-100, and protease inhibitors for 1 h on ice.

For the pull-down assay (13), the supernatant obtained by centrifugation was incubated at 48˚C for 1 h with recombinant His6-fusion RGS22 prebound to nickel-Sepharose beads under GDP^-/aberrant lateral root formation $(ALF)_4^-$ or GDP^+/ALF_4^- conditions in interaction buffer [20 mM Tris-HCl (pH 8.0), 2 mM $MgSO_4$, 6 mM β-mercaptoethanol, 100 mM NaCl, 0.05% Triton X-100, 5% glycerol]. Bound proteins were separated by 10% SDS-PAGE, and Gα subunits were visualized using antibodies against GNA12 (S-20), GNA13 (A-20) and GNA11 (C-19) (all from Santa Cruz Biotechnology) and G protein subunits (Calbiochem, San Diego, CA, USA).

For Co-IP (13), the supernatant obtained by centrifugation was incubated with recombinant His6-fusion RGS22 under GDP^-/ALF_4^- or GDP^+/ALF_4^- conditions in interaction buffer. The supernatant was then divided into two fractions and immunoprecipitated with specific anti-GNA12, anti-GNA13 and anti-GNA11 antisera, and the control antibody, followed by incubation with protein G-Sepharose. The resulting precipitates were subjected to immunoblot analysis with anti-RGS22 antibody.

Image analysis. BXPC3-LZR-GFP, BXPC3-LZR-RGS22, LZR-RGS22-Neg, LZR-RGS22-484 or LZR-RGS22-3313 cells were plated at $2x10^5$ cells in RPMI-1640 medium containing 10% FCS in a 6-well chamber slide (Lab-Tek Chambered Coverglass System; Nunc, Rochester, NY, USA) and incubated for 24 h at 37˚C. The medium was changed to serum-free RPMI-1640 medium, and cells were starved for 17 h; this was set as point 1 (0 min). LPA (final concentration, 1 μmol/l) was warmed for 5 min and added to the wells for 5, 10, 20, 30, 40 and 80 min. Cells without LPA stimulation were used as the control. Stimulation was terminated by 20-min fixation of cells with 2% paraformaldehyde. Image capture was carried out using an Axioskop 2 Plus Microscope (Carl Zeiss). LPA stimulation of BXPC-3 cells led to a 'shrunken' morphology in a proportion of cells.

If cell length was less than two times the width, the cell was defined as having a 'shrunken' morphology (round). We used the t-test for each of the two groups; $P<0.05$ was considered significant. Cells were counted according to round or stretched morphology in a blinded fashion for genotype and treatment. Each group was treated in three wells. The experiments were repeated three times.

Immunofluorescence staining for F-actin, RGS22, GNA12, GNA13, GNAq and nuclear material. LPA-stimulated BXPC3-LZR-GFP, BXPC3-LZR-RGS22, LZR-RGS22-Neg, LZR-RGS22-484 or LZR-RGS22-3313 cells (0, 1, 5, 10, 20, 30, 40 and 80 min) were permeabilized with 0.1% Triton X-100 for 1 min prior to staining. For BXPC3-LZR-GFP or BXPC3-LZR-RGS22 cells, Texas Red-X phalloidin (0.5 μM) was added into the wells and incubated for 20 min at room temperature. After washing three times with phosphate-buffered saline (PBS), cells were stained with Hoechst (1 μg/ml; Molecular Probes, Eugene, OR, USA) for 20 sec at room temperature. LZR-RGS22-Neg, LZR-RGS22-484 or LZR-RGS22-3313 cells were treated with 1:500 anti-RGS22 antibody at 4˚C overnight. After washing, cells were incubated for 1 h with 1:100 fluorescein isothiocyanate (FITC)-labeled goat anti-mouse immunoglobulin G (IgG) (Beijing Zhongshan Biotechnology). After washing with PBS, cells were stained with Texas Red-X phalloidin and Hoechst as above. After washing four times with PBS, cells were mounted with carbonate buffer solution containing 50% glycerol (pH 9.6).

BXPC3-LZR-RGS22 cells transfected by constructs each containing human Gα12 Q231L, Gα13 Q226L and Gαq Q209L in the pcDNA3.1 vector were incubated in RPMI-1640 medium containing 10% FCS for 24 h at 37˚C. The medium was changed to serum-free RPMI-1640 medium and cells were starved for 17 h; this was set as point 1 (0 min). LPA (final concentration, 1 μmol/l) was warmed for 5 min and added to the wells for 5 sec and 5 and 10 min. Cells without LPA stimulation were used as the control. Stimulation was terminated by fixing cells with 2% paraformaldehyde for 20 min, and then permeabilizing cells with 0.1% Triton X-100 for 5 min. Following 30-min rehydration with 1% BSA at room temperature, samples were incubated with antibody against GNA12, GNA13 or GNAq (1:1,000 in PBS containing 1% BSA at a final concentration of 0.2 g/ml) overnight. After washing, samples were incubated for 1 h with FITC-labeled secondary antibodies (Beijing Zhongshan Biotechnology), washed twice, incubated with 0.5 μM Texas Red-X phalloidin and Hoechst DNA stain, and then mounted as described above. The stained slides were observed under an Axioskop 2 Plus microscope (Carl Zeiss). We used uniform exposure times during photography to enable optimal comparison of fluorescence among the test samples.

Results

RGS22 overexpression inhibits BXPC-3 cell migration. Using immunohistochemical studies on a tissue microarray consisting of 96 cancer tissue types, we previously found that RGS22 is specifically expressed in adenocarcinoma and squamous carcinoma (4). In the present study, RGS22 localized to the cytoplasm in pancreatic adenocarcinoma tissues (Fig. 1). Furthermore, RGS22, a novel cancer/testis (CT) antigen, acts as a tumor suppressor, repressing epithelial cancer cell invasion and migration.

To test the effect of RGS22 expression on pancreatic adenocarcinoma cells, we overexpressed RGS22 in BXPC-3 cells. We used GFP as the control (BXPC3-LZR-GFP). Western blotting revealed 146- and 76-kDa bands; RGS22-specific antibody was expressed at a higher level in BXPC3-LZR-RGS22 cells (Fig. 2A). Cells that overexpressed RGS22 had much lower wound-healing rates than the control cells (Fig. 2B). Similarly, RGS22-overexpressing cells exhibited greatly reduced migration when compared to the control cells (Fig. 2C). Migration decreased by >50% in RGS22-overexpressing cells when compared to BXPC3-LZR-GFP cells. These results suggest that RGS22 expression suppresses pancreatic adenocarcinoma cell migration.

RGS22 downregulation in BXPC3-LZR-RGS22 cells recovered cell migration. To confirm the effect of RGS22 expression

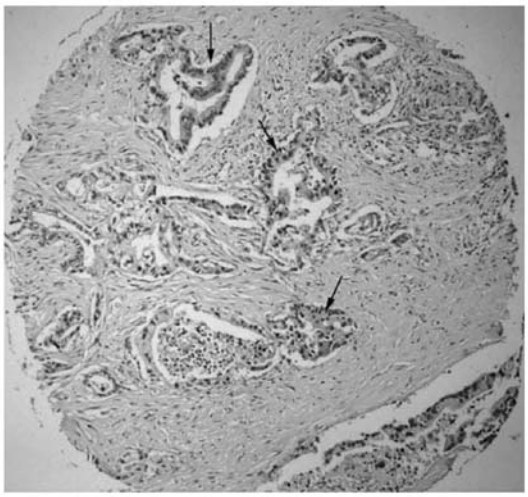

Figure 1. RGS22 expressed in pancreatic adenocarcinoma. Positive immunostaining of RGS22 in pancreatic adenocarcinoma indicated by arrows (magnification, x100).

on pancreatic adenocarcinoma cells, we downregulated RGS22 expression in BXPC3-LZR-RGS22 cells by RNA interference (RNAi) (LZR-RGS22-484 and LZR-RGS22-3313). LZR-RGS22-Neg cells were used as the control. Western blotting revealed 76-kDa bands; RGS22-specific antibody was expressed at a lower level in BXPC3-LZR-RGS22-3313 cells and at the lowest level in BXPC3-LZR-RGS22-484 cells (Fig. 3A).

BXPC3-LZR-RGS22-484 cells, in which RGS22 expression was more greatly downregulated, had higher wound-healing rates at 24 h than the control cells and BXPC3-LZR-RGS22-3313 cells (Fig. 3B); the BXPC3-LZR-RGS22-3313 cells had similar wound-healing rates to the control cells. BXPC3-LZR-RGS22-484 cell migration was greatly increased compared to the control cells (Fig. 3C). BXPC3-LZR-RGS22-484 cell migration was increased by >100% compared to that of BXPC3-LZR-RGS22-Neg cells. These results confirm that RGS22 expression suppresses pancreatic adenocarcinoma cell migration.

RGS22 interaction with GNA12/13 in BXPC-3 cells. To determine whether RGS22 interacts directly with Gα subunits in tumor cells, BXPC-3 cell lysates were incubated with fusion proteins containing His6 immobilized on nickel-Sepharose beads in the presence or absence of GDP and ALF_4^-, which mimics the transition state of the Gα subunit. RGS22 bound specifically to GNA12 and GNA13 in the cells under GDP-ALF_4^- conditions (Fig. 4A).

We confirmed the specificity of RGS22 interaction with GNA12 and GNA13 by incubating BXPC-3 cell lysates with the corresponding bead-bound antibodies under the GDP-ALF4$^-$ condition. The 146-, 112- and 76-kDa forms of RGS22 mainly bound to GNA13, while the 112-kDa form of RGS22 bound

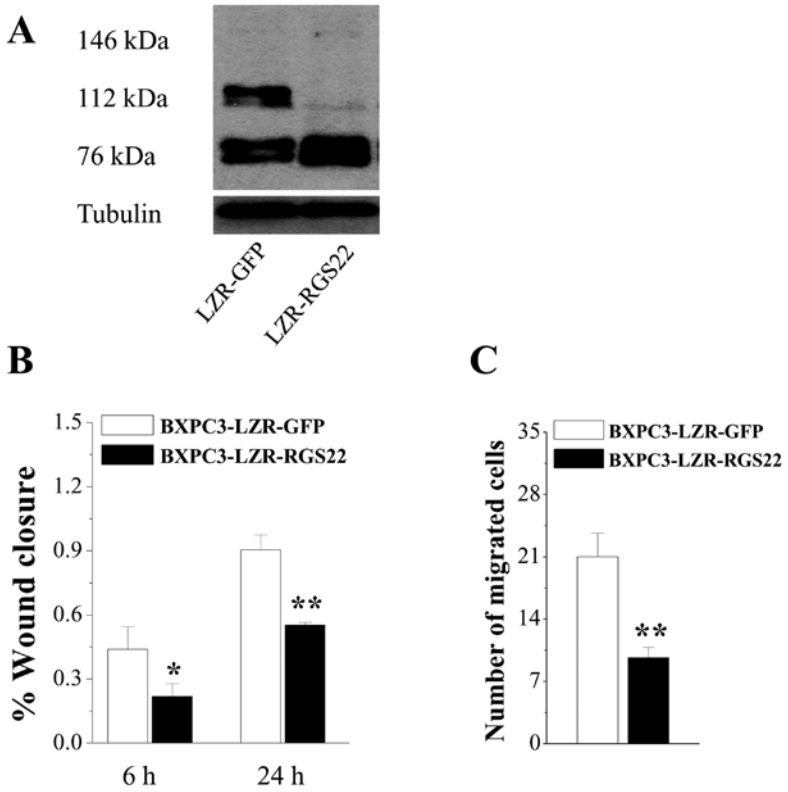

Figure 2. Migration was less in RGS22-overexpressing cells. (A) Western blot analyses of higher concentrations of 146- and 76-kDa RGS22 forms in BXPC3-LZR-RGS22 cells. BXPC3-LZR-GFP cells were used as the control. Tubulin expression in cells was used as the loading control. (B) Wound-healing assay revealed that RGS22 suppressed cell migration. The assay involved a confluent monolayer of BXPC3-LZR-GFP and BXPC3-LZR-RGS22 cells. The surrounding cells migrated into the scratched area at 6 and 24 h after scratching. Results presented are the percentage of the resettled area. (C) Transwell assay revealed that RGS22 suppressed cell migration. Data presented are the mean ± SE of three Transwell filters from a single experiment. RGS22 suppressed migration in BXPC3-LZR-RGS22 cells relative to the control BXPC3-LZR-GFP cells. $^*P<0.05$ and $^{**}P<0.01$.

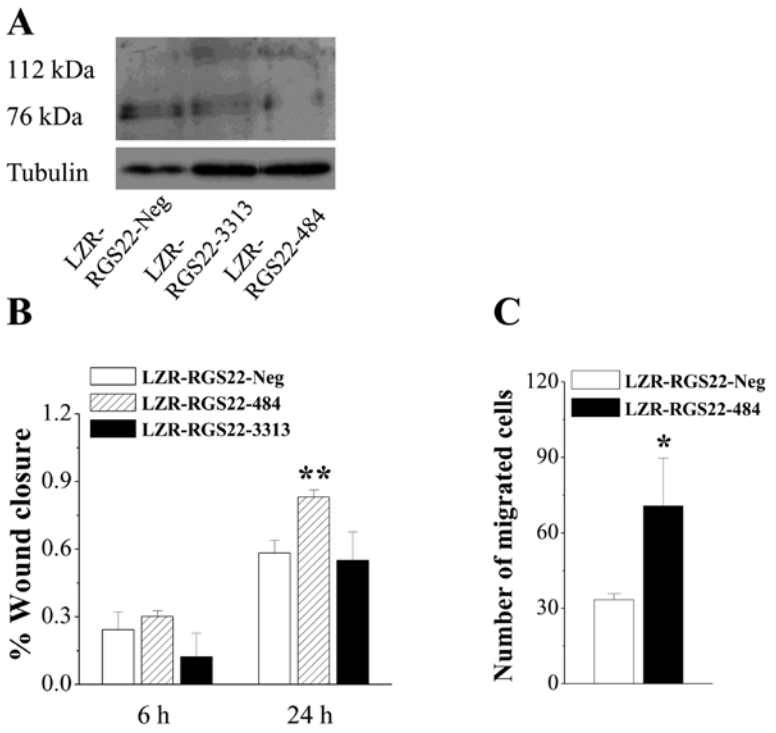

Figure 3. Migration was higher in RGS22-downregulated cells. (A) Western blot analyses showing lower concentrations of the 76-kDa RGS22 form in LZR-RGS22-3313 cells; concentration was lowest in LZR-RGS22-484 cells. LZR-RGS22-Neg cells were used as the control. Tubulin expression was used as the loading control. (B) Wound-healing assay revealed that downregulating RGS22 promoted cell migration. The assay involved a confluent monolayer of LZR-RGS22-Neg, LZR-RGS22-3313 and LZR-RGS22-484 cells. The surrounding cells migrated into the scratched area at 6 and 24 h after scratching. Results presented are the percentage of the resettled area. (C) Transwell assay revealed that downregulating RGS22 promoted cell migration. Data are presented as the mean ± SE of three Transwell filters from a single experiment. RGS22 downregulation promoted migration of LZR-RGS22-484 cells relative to the control LZR-RGS22-Neg cells. *P<0.05 and **P<0.01.

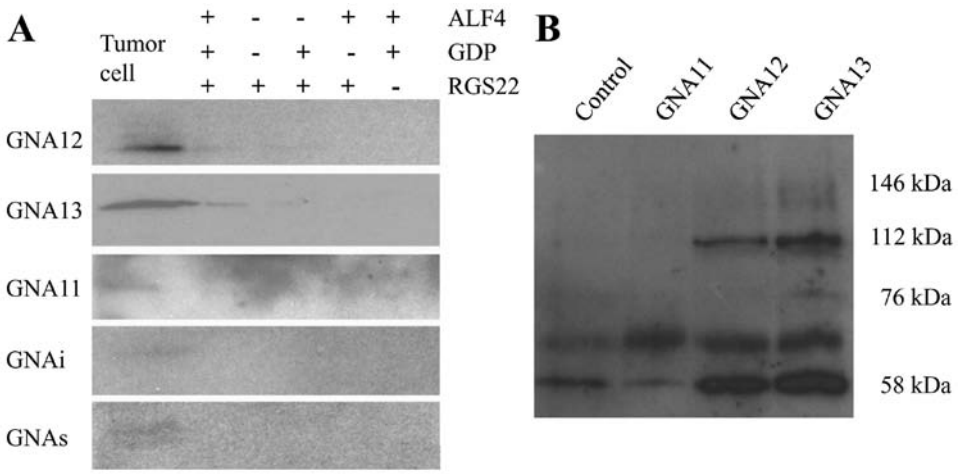

Figure 4. RGS22 interactions with Gα12 and Gα13. (A) Interactions between RGS22 and Gα subunits. Extracted proteins were immunoblotted for the various Gα subunits. BXPC-3 cell lysates were used as the positive control. (B) Co-IP of RGS22 and Gα subunits 12, 13 and q/11. The 146-, 112- and 76-kDa forms of RGS22 were co-immunoprecipitated with GNA13; the 112-kDa form of RGS22 was co-immunoprecipitated with GNA12. However, RGS22 did not interact with GNA11.

primarily to GNA12. RGS22 did not bind to GNAq/11. The 59-kDa form of RGS22 may have been masked by the heavy chain of IgG (Fig. 4B). These data indicate that RGS22 has specific interactions with GNA12 and GNA13 in BXPC-3 cells.

RGS22 inhibits LPA-activated pancreatic cancer cell morphological changes and F-actin formation. LPA is a small bioactive phospholipid produced by some cancer cells (14). It is involved in a variety of physiological and pathophysiological responses, including wound healing and tumor cell invasion and metastasis (15). Several G protein-coupled receptors mediate the biological functions of LPA. LPA interacts with receptors LPA1-5, which in turn activate the Gi, Gq, Gs/h and G12/13 proteins to elicit multiple biological responses.

To characterize the RGS22-induced decrease in BXPC-3 cell migration, we examined the morphology of LPA-stimulated

live cells. We used BXPC3-LZR-RGS22 cells stably transfected with full-length human RGS22 or GFP-tagged BXPC3-LZR-GFP cells. The control BXPC3-LZR-GFP cells began to appear rounded 5 min after LPA stimulation, while BXPC3-LZR-RGS22 cells began to shrink 20 min after LPA stimulation. The images obtained showed that the control cells achieved the maximum rate of cell deformation 20 min after LPA stimulation. However, the BXPC3-LZR-RGS22 cells achieved the maximum rate of cell deformation only after 30 min (Fig. 5A and B). Downregulating RGS22 expression reversed its inhibitory effect on BXPC3-LZR-RGS22-484 cells compared to the BXPC3-LZR-RGS22-Neg cells. The reaction began at 5 min, and the time taken to achieve the maximum deformation cell ratio was 20 min (Fig. 5A and C). So, the higher the RGS22 expression, the later the cell deformation after LPA stimulation.

The actin cytoskeleton has been implicated in the management of cell shape and migration activity (16). To determine whether RGS22 involves LPA-mediated F-actin polymerization, we triple-stained cells with Hoechst (stains nuclei blue), RGS22-specific antibody (control cells were tagged with GFP, green), and Texas Red-X phalloidin (stains F-actin red). LPA induced the formation of a dense and organized network of thick, parallel F-actin stress fibers starting at 1 min in BXPC3-LZR-GFP cells (Fig. 5A). In BXPC3-LZR-RGS22 cells, in which RGS22 expression was higher, LPA-induced F-actin stress fiber formation was delayed to 10 min (Fig. 5A). Downregulating RGS22 expression recovered its inhibitory effect on BXPC3-LZR-RGS22-484 cells compared to BXPC3-LZR-RGS22-Neg cells (Fig. 5A). LPA-induced F-actin stress fiber formation was delayed to 10 min in BXPC3-LZR-RGS22-484 cells. Therefore, our studies demonstrate that higher RGS22 expression delays LPA-induced F-actin formation.

Effect of constitutive activation of Gα subunits by RGS22 on LPA-activated morphological changes and F-actin formation. We used LZR-RGS22 BXPC-3 cells transiently transfected with constructs containing human Gω12 Q231L, Gα13 Q226L or Gαq Q209L to test whether RGS22 inhibits F-actin formation through the Gα12, Gα13 or Gαq subunit. These mutations reduce guanosine triphosphatase (GTPase) activity, resulting in a constitutively active phenotype with or without RGS proteins. That is, RGS proteins bind to constitutively active Gα subunits without accelerating GTP hydrolysis to GDP. We did not investigate the function of RGS proteins as negative regulators of heterotrimeric G protein signaling.

Cells were triple stained with Hoechst (blue), Gα subunit-specific antibody (green), and Texas Red-X phalloidin. Cells transfected with Gα12 Q231L and Gα13 Q226L began to appear rounded and F-actin stress fibers began to form 5 sec after LPA stimulation. F-actin stress fiber formation in untransfected cells and Gαq Q209L-transfected cells (Fig. 6) began 10 min after LPA stimulation.

Discussion

Several features of pancreatic cancer are responsible for the high mortality rate; it is difficult to detect precursor lesions or notice symptoms until the disease is in the advanced stages (17). Pancreatic cancer often undergoes micrometastasis, which is responsible for its poor prognosis. In a previous study, we showed that RGS22 localized to the cytoplasm in pancreatic adenocarcinoma tissues, indicating its association with pancreatic adenocarcinoma. We also found that RGS22 expression is higher in cancers without lymph node metastasis than in cancers with lymph node metastasis. RGS22 can inhibit tumor metastasis. To confirm this, we used the human pancreatic cancer cell line BXPC-3 to test the association of RGS22 with pancreatic cancer cell migration. BXPC3-LZR-RGS22 cells, with higher RGS22 expression, had lower wound-healing rates and migration than BXPC3-LZR-GFP control cells. Conversely, downregulating RGS22 in BXPC3-LZR-RGS22-484 cells resulted in higher wound-healing rates and migration than in BXPC3-LZR-RGS22-Neg control cells. Therefore, RGS22 is inhibitory toward human pancreatic cancer cell migration.

Several classes of proteins are involved in cell migration and metastasis. GNA12 signaling promotes cell migration in prostate (9) and breast cancer (10), and in LPA-induced ovarian cancer cells *in vitro* (11). In these studies, Rho activation appeared critical to the effect of GNA12 in promoting invasion. GNA12 signaling promoting metastasis takes place via the stimulation of cells to become invasive within the primary tumor. GNA13 also stimulates cell migration in addition to inducing oncogenic transformation (12). Via pull-down and Co-IP assays, we found that RGS22 interacted with GNA12/13.

Increased cell migration is an acquired feature of metastatic cancer cells. Cell migration is an important component in the spread of pancreatic cancer (18). In the early stages of the disease, cancer spread is believed to occur after tumor cells infiltrate the peritoneal cavity and gain access to the blood vessels. Thus, studying the migratory abilities of pancreatic cancer cells is necessary for providing insight into the biological processes that mediate metastasis. One of the simplest natural phospholipids, LPA is a lipid mediator that evokes hormone- and growth factor-like responses in almost every cell type. LPA is an efficacious chemoattractant of human pancreatic carcinoma cells (19). In the malignant ascites from pancreatic cancer patients, LPA is an active component that stimulates pancreatic cancer cell migration and invasion. We used LPA as a stimulator to investigate the possible mechanism of RGS22 in pancreatic cancer cell migration. LPA stimulation led to altered cell morphology; BXPC3-LZR-RGS22 cells began to appear rounded and achieved the maximum rate of cell deformation more quickly after stimulus than control cells. Furthermore, the downregulated RGS22 expression in BXPC3-LZR-RGS22-484 cells recovered the inhibitory effect of RGS22 compared to BXPC3-LZR-RGS22-Neg cells.

Migrating cells are crucial for accurate organization of the actin cytoskeleton and the migratory response of pancreatic carcinoma cells (20). To determine whether RGS22 is involved in LPA-mediated F-actin polymerization, we triple-stained the cells. In the high-RGS22 expression BXPC3-LZR-RGS22 cells, F-actin stress fiber formation was delayed compared to BXPC3-LZR-GFP cells. The inhibitory effect of RGS22 was recovered by downregulating RGS22 expression in BXPC3-LZR-RGS22-484 cells compared to BXPC3-LZR-RGS22-Neg cells. Therefore, our studies demonstrate that higher RGS22 expression delays LPA-induced F-actin formation.

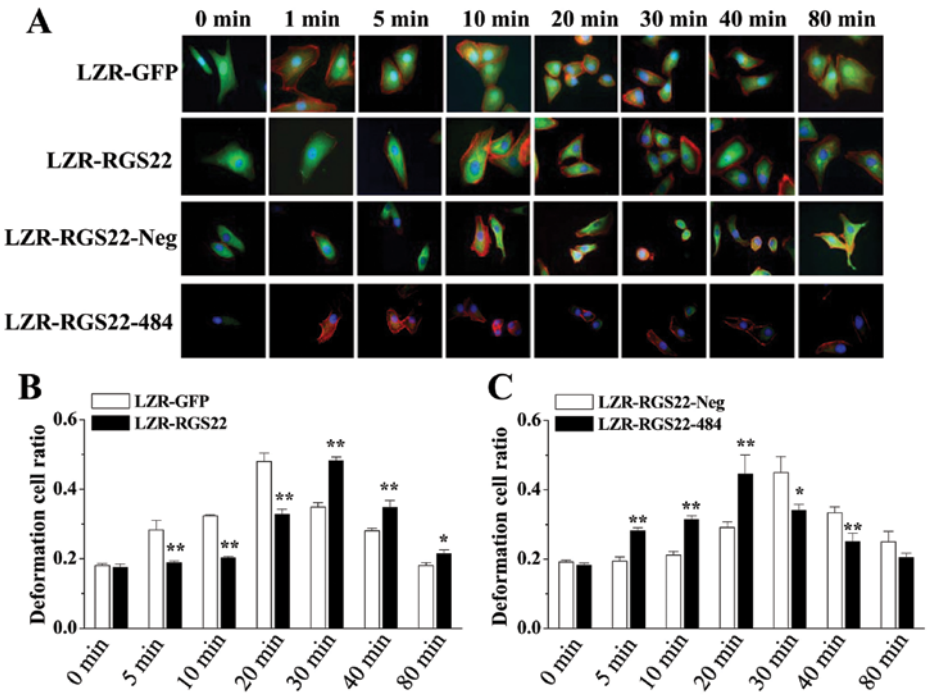

Figure 5. RGS22 inhibits LPA-activated pancreatic cancer cell morphological changes and F-actin formation. (A) RGS22 delayed LPA-stimulated F-actin formation and cell deformation. LPA-activated F-actin formation in BXPC3-LZR-GFP cells. F-actin (red) began to form thick fibers 1 min after LPA stimulus; GFP (green) was expressed throughout the cell; Hoechst stained the nuclei blue (magnification, x1,000). Cells start to be round after 5 min LPA stimulation. While, the F-actin (red) reaction began 5 min after LPA stimulus in RGS22 (green, anti-RGS22 antibody) high expressed BXPC3-LZR-RGS22 cells and cells begin to shrink 20 min after stimulation. F-actin (red) began to form thick fibers 10 min after LPA stimulus in LZR-RGS22-Neg cells. RGS22 (green) is expressed in the cytoplasm; Hoechst stained the nuclei blue (magnification, x1,000). Cells start to be round after 20 min LPA stimulation While, F-actin (red) began to form thick fibers in 1 min, in LZR-RGS22-484 cells after LPA stimulus and cells begin to shrink 5 min after stimulation. (B) RGS22 inhibition of LPA-activated pancreatic cancer cell morphological changes. y-axis, ratio of deformation cells. RGS22 delayed LPA-stimulated cell deformation. The reaction began 5 min after LPA stimulus in BXPC3-LZR-GFP cells and 20 min in BXPC3-LZR-RGS22 cells. Maximum cell deformation rates after LPA stimulus occurred after 20 min in BXPC3-LZR-GFP cells and 30 min in BXPC3-LZR-RGS22 cells. Each of the two groups was analyzed by t-test. *P<0.05 and **P<0.01. (C) Downregulated RGS22 accelerates LPA-activated pancreatic cancer cell morphological changes. y-axis, ratio of deformation cells. Cell deformation reaction began 20 min after LPA stimulus in LZR-RGS22-Neg cells and 5 min in RGS22 downregulated LZR-RGS22-484 cells. Maximum cell deformation rates after LPA stimulus occurred after 30 min in LZR-RGS22-Neg cells and 20 min in LZR-RGS22-484 cells. Each of the two groups was analyzed by t-test. *P<0.05 and **P<0.01.

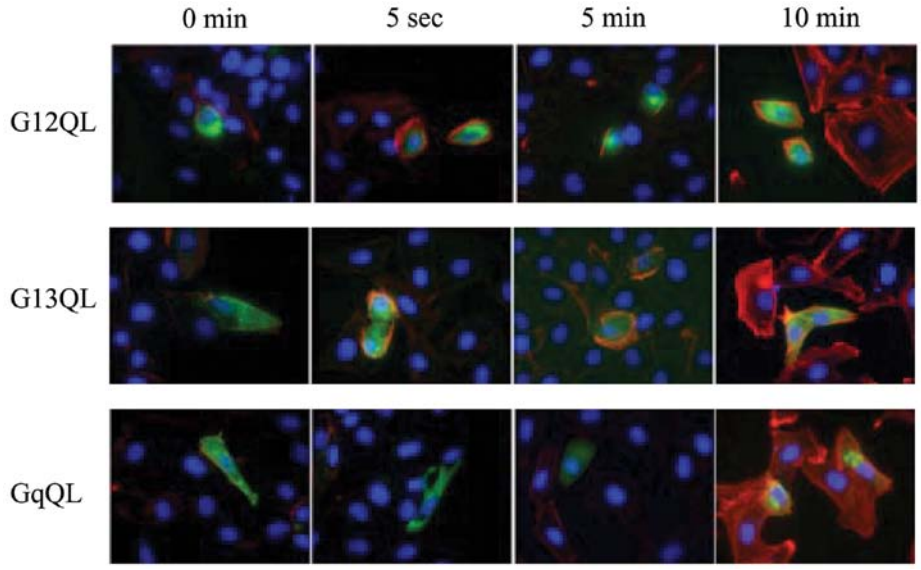

Figure 6. Expression of constitutively active Gα12 and Gα13 but not constitutively active Gαq in BXPC3-LZR-regulator of G protein signaling 22 (RGS22) cells inhibit RGS22 signaling. Cell deformation and F-actin (red) formation of thick fibers began after 5 sec in cells into which constitutively active Gα12 (green) had been transferred. Gα12 (green) is expressed in the cytoplasm and cell membrane. F-actin (red) began to form thick fibers after 10 min in cells into which constitutively active Gα12 had not been transferred. Nuclei are stained blue (magnification, x1,000). Furthermore, cell deformation and F-actin (red) formation of thick fibers began after 5 sec in cells into which constitutively active Gα13 (green) had been transferred. Gα13 (green) is expressed in the cytoplasm and cell membrane. F-actin (red) began to form thick fibers after 10 min in cells into which constitutively active Gα13 had not been transferred. Nuclei are stained blue (magnification, x1,000). While, F-actin (red) began to form thick fibers after 10 min in cells into which constitutively active Gαq (green) had, and had not been transferred. Gαq (green) is expressed in the cytoplasm and cell membrane. Nuclei are stained blue (magnification, x1,000).

The G12/13 G protein family has been implicated in various cellular processes, such as Rho-mediated organization of the cytoskeleton, and subsequently, cell shape (21). G12/13-mediated stress fiber formation is important for cell motility. The complex interplay of actin polymerization orchestrates cell movement. We inhibited RGS22 signaling by expressing constitutively active GNA12 and GNA13 (but not GNAq) in BXPC3-LZR-RGS22 cells. These results further support the notion of RGS22 signaling, whereby RGS22 couples to GNA12/13, which in turn inhibits stress fiber formation.

In conclusion, our data demonstrate that RGS22 acts as a tumor suppressor, repressing human pancreatic adenocarcinoma cell migration by coupling to GNA12/13, which in turn leads to the inhibition of stress fiber formation. RGS22 may be a promising therapeutic target for tumor metastasis pathway intervention.

Acknowledgements

This study was supported by grants from the Six Talent Peaks Project of Jiangsu Province of China (no. 2013-WSN-021), the 333 Project of Jiangsu Province of China, the Key Medical Talents of Yangzhou City, the National Natural Science Foundation of China (NSFC) (no. 81200127), and the Natural Science Foundation of Jiangsu Province of China (no. BK20131230).

References

1. Bardeesy N, Sharpless NE, DePinho RA and Merlino G: The genetics of pancreatic adenocarcinoma: A roadmap for a mouse model. Semin Cancer Biol 11: 201-218, 2001.
2. Zhang XJ, Ye H, Zeng CW, He B, Zhang H and Chen YQ: Dysregulation of miR-15a and miR-214 in human pancreatic cancer. J Hematol Oncol 3: 46, 2010.
3. Hu Y, Xing J, Chen L, Guo X, Du Y, Zhao C, Zhu Y, Lin M, Zhou Z and Sha J: RGS22, a novel testis-specific regulator of G-protein signaling involved in human and mouse spermiogenesis along with GNA12/13 subunits. Biol Reprod 79: 1021-1029, 2008.
4. Hu Y, Xing J, Wang L, Huang M, Guo X, Chen L, Lin M, Zhou Y, Liu Z, Zhou Z, *et al*: RGS22, a novel cancer/testis antigen, inhibits epithelial cell invasion and metastasis. Clin Exp Metastasis 28: 541-549, 2011.
5. Fokas E, Engenhart-Cabillic R, Daniilidis K, Rose F and An HX: Metastasis: The seed and soil theory gains identity. Cancer Metastasis Rev 26: 705-715, 2007.
6. Liotta LA, Steeg PS and Stetler-Stevenson WG: Cancer metastasis and angiogenesis: An imbalance of positive and negative regulation. Cell 64: 327-336, 1991.
7. Orr FW, Wang HH, Lafrenie RM, Scherbarth S and Nance DM: Interactions between cancer cells and the endothelium in metastasis. J Pathol 190: 310-329, 2000.
8. Hu J and Verkman AS: Increased migration and metastatic potential of tumor cells expressing aquaporin water channels. FASEB J 20: 1892-1894, 2006.
9. Kelly P, Stemmle LN, Madden JF, Fields TA, Daaka Y and Casey PJ: A role for the G12 family of heterotrimeric G proteins in prostate cancer invasion. J Biol Chem 281: 26483-26490, 2006.
10. Kelly P, Moeller BJ, Juneja J, Booden MA, Der CJ, Daaka Y, Dewhirst MW, Fields TA and Casey PJ: The G12 family of heterotrimeric G proteins promotes breast cancer invasion and metastasis. Proc Natl Acad Sci USA 103: 8173-8178, 2006.
11. Bian D, Mahanivong C, Yu J, Frisch SM, Pan ZK, Ye RD and Huang S: The G12/13-RhoA signaling pathway contributes to efficient lysophosphatidic acid-stimulated cell migration. Oncogene 25: 2234-2244, 2006.
12. Radhika V, Onesime D, Ha JH and Dhanasekaran N: Galpha13 stimulates cell migration through cortactin-interacting protein Hax-1. J Biol Chem 279: 49406-49413, 2004.
13. Mao H, Zhao Q, Daigle M, Ghahremani MH, Chidiac P and Albert PR: RGS17/RGSZ2, a novel regulator of Gi/o, Gz, and Gq signaling. J Biol Chem 279: 26314-26322, 2004.
14. Choi KU, Yun JS, Lee IH, Heo SC, Shin SH, Jeon ES, Choi YJ, Suh DS, Yoon MS and Kim JH: Lysophosphatidic acid-induced expression of periostin in stromal cells: Prognoistic relevance of periostin expression in epithelial ovarian cancer. Int J Cancer 128: 332-342, 2011.
15. Yatomi Y, Igarashi Y, Yang L, Hisano N, Qi R, Asazuma N, Satoh K, Ozaki Y and Kume S: Sphingosine 1-phosphate, a bioactive sphingolipid abundantly stored in platelets, is a normal constituent of human plasma and serum. J Biochem 121: 969-973, 1997.
16. Roffers-Agarwal J, Xanthos JB and Miller JR: Regulation of actin cytoskeleton architecture by Eps8 and Abi1. BMC Cell Biol 6: 36, 2005.
17. Yadav D and Lowenfels AB: The epidemiology of pancreatitis and pancreatic cancer. Gastroenterology 144: 1252-1261, 2013.
18. Doi Y, Yashiro M, Yamada N, Amano R, Noda S and Hirakawa K: VEGF-A/VEGFR-2 signaling plays an important role for the motility of pancreas cancer cells. Ann Surg Oncol 19: 2733-2743, 2012.
19. Yamada T, Sato K, Komachi M, Malchinkhuu E, Tobo M, Kimura T, Kuwabara A, Yanagita Y, Ikeya T, Tanahashi Y, *et al*: Lysophosphatidic acid (LPA) in malignant ascites stimulates motility of human pancreatic cancer cells through LPA1. J Biol Chem 279: 6595-6605, 2004.
20. Hage B, Meinel K, Baum I, Giehl K and Menke A: Rac1 activation inhibits E-cadherin-mediated adherens junctions via binding to IQGAP1 in pancreatic carcinoma cells. Cell Commun Signal 7: 23, 2009.
21. Offermanns S: G-proteins as transducers in transmembrane signalling. Prog Biophys Mol Biol 83: 101-130, 2003.